The Role of Convectively Coupled Atmospheric Kelvin Waves on African Easterly Wave Activity

MICHAEL J. VENTRICE AND CHRIS D. THORNCROFT

Department of Atmospheric and Environmental Science, University at Albany, State University of New York, Albany, New York

(Manuscript received 16 May 2012, in final form 24 October 2012)

ABSTRACT

The role of convectively coupled atmospheric Kelvin waves (CCKWs) on African easterly wave (AEW) activity is explored over tropical Africa during boreal summer. Examination of the pre-Alberto AEW in 2000 highlights the observation that the convective trigger for the initiation of the AEW was generated by a strong CCKW and that the subsequent intensification of the AEW at the West African coast was associated with a second CCKW. Composite analysis shows that, generally, AEW activity increases during and after the passage of the convectively active phase of strong CCKWs. The increase in AEW activity is consistent with convective triggering at the leading edge of the convective phase of the CCKW. This convective triggering occurs in a region where the background low-level easterly vertical wind shear is increased by the CCKW. As the AEW propagates westward through the convectively active phase of the CCKW, it can develop in an environment favorable for convection. It is also shown that this phase of the CCKW is characterized by enhanced meridional vorticity gradients in the core of the African easterly jet suggesting that enhanced mixed barotropic–baroclinic growth may also be responsible for enhanced AEW activity there.

1. Introduction

The impact of African easterly waves (AEWs) on West African rainfall during boreal summer is a well-known and extensively studied topic (e.g., Kiladis et al. 2006 and references therein). In addition to having a strong impact on West African rainfall, AEWs can also act as initial precursors for tropical cyclones over the tropical Atlantic (e.g., Avila and Pasch 1992) and over the Pacific (Frank 1970) Oceans. Given the large body of work on these waves, it is perhaps surprising that there is still a lack of understanding of when and how these waves originate. During the 1970s, most believed that AEWs formed from a mixed barotropic and baroclinic instability mechanism, which was backed by several idealized modeling studies showing that AEWs could grow from small amplitudes on an unstable African easterly jet (AEJ; e.g., Rennick 1976; Simmons 1977; Thorncroft and Hoskins 1994a,b). Recent work has challenged this hypothesis (e.g., Mekonnen et al. 2006; Hall et al. 2006; Thorncroft et al. 2008). These studies have proposed that AEWs are triggered by convection in the entrance region of the AEJ. Thorncroft et al. (2008) suggest that AEWs rely on the presence of intense upstream convective triggers linked to African topography. We argue here that convectively coupled equatorial atmospheric Kelvin waves (CCKWs) can provide such triggers over African topography by providing a favorable environment for convection and wave growth. This concept provides new insight on a concept that is not yet fully understood and could ultimately be used to support medium-range prediction of AEW activity.

Synoptic case study work of Carlson (1969a) and, more recently, Berry and Thorncroft (2005) highlighted the role of orographic convection in triggering AEWs. Berry and Thorncroft (2005) suggested that the strong AEW that developed into Hurricane Alberto (2000) was triggered by strong convection over the Darfur Mountains (~25°E) on 30–31 July 2000. In a climatological study of AEW activity, Mekonnen et al. (2006) also noted the importance of the eastern African highlands on AEW genesis. In agreement with Berry and Thorncroft (2005), they found that the Darfur Mountains and the Ethiopian Highlands (~35°E) are both preferable regions for AEW genesis. This triggering hypothesis was

Corresponding author address: Michael Ventrice, University at Albany, State University of New York, 1400 Washington Ave., Albany, NY 12222.
E-mail: mventrice@albany.edu

DOI: 10.1175/MWR-D-12-00147.1

also supported by idealized modeling of Thorncroft et al. (2008). While the model they used had a flat lower boundary, the atmospheric response to imposed upstream heating in the Darfur region (close to the entrance of the African easterly jet) was a developing train of AEWs that propagated westward with time, providing strong evidence in support of the triggering hypothesis. It will be shown here that the increased convection linked to the genesis of the pre-Alberto AEW over the Darfur Mountains occurred during the passage of the convectively active phase of a strong eastward-propagating CCKW.

While this paper mainly focuses on the triggering of AEWs by convection associated with the convectively active phase of the CCKW, it should be recognized that convection can also impact the presence and amplitude of AEW activity through, at least, two other mechanisms. Schubert et al. (1991) highlighted the role played by the intertropical convergence zone (ITCZ) heating in the creation of a zonally symmetric potential vorticity (PV) strip that is unstable for AEW growth (see also Hsieh and Cook 2005). Numerous studies have also shown that convection and associated heating coupled with the AEW itself can intensify preexisting AEWs (e.g., Thorncroft and Hoskins 1994a,b; Hsieh and Cook 2008). Unraveling the relative roles played by convection on the genesis and growth or maintenance of AEWs is difficult and likely requires a modeling study that is beyond the scope of this paper.

CCKWs substantially modulate tropical convection in the region of the ITCZ on synoptic spatial and temporal scales (Gruber 1974; Zangvil 1975; Takayabu 1991; Pires et al. 1997; Wheeler and Kiladis 1999; Wheeler et al. 2000; Mounier et al. 2007; Mekonnen et al. 2008; Laing et al. 2011; Ventrice et al. 2012a). Observational studies using high resolution rainfall and brightness temperature datasets [e.g., *Geostationary Operational Environmental Satellite-9* (*GOES-9*), the Cloud Archive Service (CLAUS), and the Tropical Rainfall Measuring Mission (TRMM) product 3B42] reveal that most of the organized rainfall within the convective envelope of the CCKW comprises smaller-scale cloud clusters that move westward (e.g., Straub and Kiladis 2002; Mounier et al. 2007; Mekonnen et al. 2008; Kiladis et al. 2009; Schreck and Molinari 2011; Laing et al. 2011; Tulich and Kiladis 2012). Mounier et al. (2007) observed an increase of mesoscale convective system (MCS) activity within the convective envelope of a CCKW over Africa during early July 1984. Their results show that CCKWs are able to modulate convective activity over the whole ITCZ domain by impacting the frequency and intensity of MCSs, with an emphasis over the Cameroon Highlands and central Africa. Nguyen and Duvel (2008) and Laing et al. (2011) also find that MCSs are more frequent, larger, and more intense within the convective envelope of CCKWs.

Mekonnen et al. (2008) observed an increase in AEW activity directly after the passage of a strong CCKW passage over Africa during the boreal summer of 1987. However, Mekonnen et al. (2008) suggests that this case was a rare event, stating that on average only three AEWs initiate per year over Africa during the passage a CCKW. In support of CCKWs modulating AEW activity, Leroux et al. (2010) suggested that intraseasonal variability of AEW activity can vary with eastward-propagating modes such as CCKWs and the Madden–Julian oscillation (MJO). These eastward-propagating disturbances are suggested to impact convection and the characteristics of the AEJ over Africa, which thereafter would impact AEW activity. Using Wheeler and Hendon's (2004) Real-time Multivariate MJO indices, Ventrice et al. (2011) and Alaka and Maloney (2012) showed that the MJO does indeed impact AEW activity through its impact on upstream convection and the AEJ. A follow-up to this analysis is presented and considers the role of strong CCKWs.

Matthews (2004) showed that African convection strongly varies at intraseasonal time scales and attributed the dominant mode of variability to the superposition between a dry westward-propagating equatorial Rossby wave response and a dry eastward-propagating Kelvin wave response over Africa. Both the dry Rossby and Kelvin wave responses originated from active convection associated with the MJO over the west Pacific warm pool, which then propagated around the globe and intersected over Africa 20 days later. The dry Kelvin wave response destabilized the atmosphere, increased the surface monsoon flow and moisture supply into West Africa up to 20%, and increased the cyclonic shear on the equatorward flank of the AEJ. The increased cyclonic shear on the equatorward flank of the AEJ enhanced the instability of the jet and was attributed by the author to cause a period of enhanced AEW and transient convective activity.

In summary, this paper is motivated by the hypothesis of Mekonnen et al. (2008) that CCKWs could act as convective triggers for AEWs. This hypothesis differs from that proposed by Matthews (2004), since we investigate the impact of a moist Kelvin wave on the large-scale environment that favors AEW activity. We hypothesize that enhanced convection, triggered by CCKWs, is important for the initiation of AEWs over Africa. This work will extend that of Mekonnen et al. (2008) and provide further details on how CCKWs affect AEW genesis and growth.

This paper is constructed as follows. Section 2 discusses the datasets and methodology used. Section 3 considers the role of a CCKW on the initiation of the AEW that later formed into Hurricane Alberto (2000). A composite analysis that investigates the role of CCKWs on atmospheric parameters associated with AEW genesis and intensification is in section 4. Discussion and conclusions are included in section 5.

2. Data and methodology

The European Centre for Medium-Range Weather Forecasts (ECMWF) Re-Analysis Interim (ERA-Interim) dataset (Dee et al. 2011) was used to investigate the impact of a CCKW passage on the synoptic environment over tropical Africa. This study uses the 1.5° gridded horizontal resolution version covering the period from 1989 to 2009.

Tropical rainfall information associated with the pre-Alberto AEW case study is provided by the TRMM Multisatellite Precipitation Analysis (TMPA; TRMM product 3B42; Huffman et al. 2007). This dataset merges precipitation estimates from passive microwave sensors on a set of low-Earth-orbiting satellites that are calibrated using global analyses of monthly rain gauge data. This dataset is made available from 1998 to the present on 3-hourly 0.25° latitude–longitude grids, but has been averaged to 6-hourly 1° latitude–longitude grids to improve computational efficiency. By averaging the data onto a coarser grid, the missing data were interpolated bilinearly in space and linearly in time from the surrounding values [see Schreck et al. (2011) for more details].

Geostationary Earth orbit infrared radiation (IR) data from the Climate Prediction Center (CPC) merged IR dataset were used to investigate the convective burst over Darfur that has been attributed to as the initiation of the pre-Alberto AEW (Berry and Thorncroft 2005). The CPC-merged IR dataset is a composite of all geostationary Earth-orbiting IR ($\sim$11 μm) images from the Multifunctional Transport Satellite (MTSAT; formerly the geostationary meteorological satellite), GOES, and Meteosat satellites (Janowiak et al. 2001). Zenith angle corrections are used to match brightness temperatures away from the respective subsatellite points. This data are made available at 4-km spatial resolution every 30 min.

Following Leroux et al. (2010), AEW activity was diagnosed by calculating the eddy kinetic energy (EKE) based on ECMWF-Interim wind data that were filtered in a 2–10-day band (u' and v'). The EKE is defined as

$$\mathrm{EKE} = \frac{1}{2}(u'^2 + v'^2) \tag{1}$$

and was calculated at the level of the AEJ (700 hPa).

The CCKWs used in the composite analysis were identified by filtering National Oceanic and Atmospheric Administration's (NOAA's) daily averaged interpolated OLR dataset (e.g., Liebmann and Smith 1996) in wavenumber and frequency within the Kelvin band [a period of 2.5–20 days, with eastward wavenumbers 1–14, constrained by the Kelvin wave dispersion curves for equivalent depths of 8–90 m; see Wheeler and Kiladis (1999) for additional details]. This methodology has been demonstrated successfully in past work (e.g., Straub and Kiladis 2002; Mekonnen et al. 2008). In short, this methodology decomposes a field of data into wavenumber-frequency components for eastward-moving wave disturbances. Before the decomposition, the data are detrended and the ends of the time series were tapered to zero to control spectral leakage.

Following the methodology of Ventrice et al. (2012a,b), an index (hereafter the CCKW index) was developed by selecting all dates between June–September (JJAS) 1989 and 2009 when the minimum negative Kelvin-filtered OLR anomaly (less than -1.5 standard deviations in magnitude) was over a selected grid point (10°N, 15°W). We pick the same grid point as Ventrice et al. (2012a,b) for consistency. A total of 142 CCKWs were objectively identified using this methodology. Lags were then used on this time series in order to examine propagating characteristics. For clarification, ''day 0'' is when the minimum negative Kelvin-filtered OLR anomaly moves over the selected base point.

Anomalies for all composited fields were constructed by subtracting the long-term mean and the first four harmonics of the seasonal cycle. Bootstrap random resampling tests with 1000 iterations were used for statistical significance testing on all anomalies similar to Roundy and Frank (2004). In each of these tests, a new sample equal in size to the original was randomly drawn for the original set of composite dates with replacement. The composite anomalies were considered 95% significant if 950 out of the 1000 random composites had the same sign. All figures were made using the National Center for Atmospheric Research (NCAR) Command Language (NCL), version 6.0.0 (Brown et al. 2012). The space–time filtering technique described above was performed using NCL.

3. The influence of a convectively coupled Kelvin wave on the initiation of the pre-Alberto African easterly wave (2000)

A time–longitude plot of unfiltered TRMM 3B42 rain-rate anomalies and Kelvin-filtered TRMM rain-rate anomalies is used to highlight the role of CCKWs on the pre-Alberto AEW (Fig. 1). Only the $\pm$2 mm day^{-1}

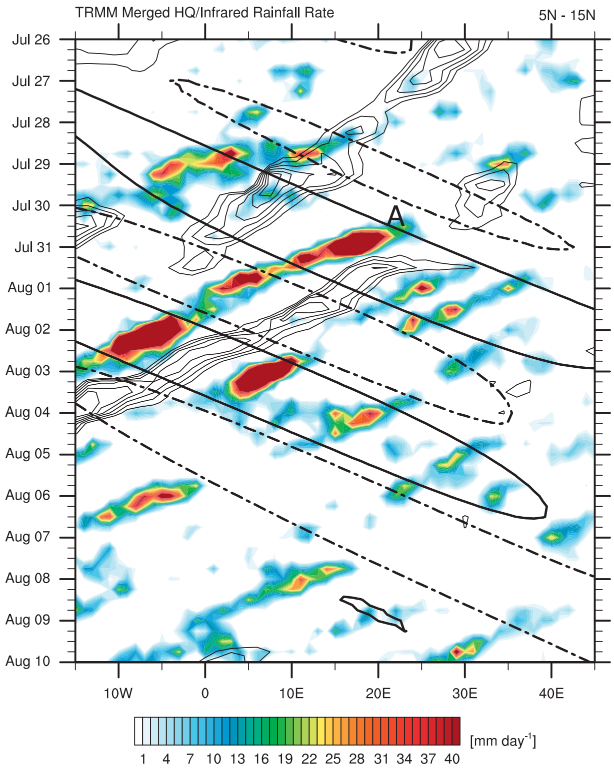

FIG. 1. A time–longitude plot of unfiltered rain-rate anomalies (positive anomalies shaded) overlaid with Kelvin-filtered rain-rate anomalies (contoured) averaged between the 5° and 15°N band for the period of 20 Jul–10 Aug 2000. The initiation of the MCS linked to the genesis of the pre-Alberto AEW is denoted as ''A.'' The ± 2 mm day^{-1} Kelvin-filtered rain-rate anomaly is only contoured to indicate each phase of the CCKW. Positive values of total meridional wind are contoured (black), the contouring begins at 2 m s^{-1}, and the contour interval is 1 m s^{-1}.

Kelvin-filtered TRMM rain-rate anomaly contour is shown to reference the location of strong CCKWs. ERA-Interim southerly winds at the level of the AEJ (700 hPa) are contoured black if greater than 2 m s^{-1} to indicate southerly flow associated with the circulation of AEWs. All variables were averaged over the 5°–15°N latitude band. The letter ''A'' represents the time and location of the 30 July convective burst over the Darfur Mountains (20°–30°E) that has been attributed to the genesis of the pre-Alberto AEW (Berry and Thorncroft 2005). The circulation associated with the pre-Alberto AEW began 1 day after this convective burst (31 July). While the dynamical signature associated with the pre-Alberto AEW shows gradual intensification during its westward propagation over tropical Africa, consistent with the observations of Berry and Thorncroft (2005), its rain-rate signature reveals distinct periods of strengthening and weakening. The strengthening and weakening of the pre-Alberto AEW rain-rate signature has not been discussed in previous studies and appears to be related to the passage of the convectively active and suppressed phases of consecutive eastward-propagating CCKWs.

Between 27 July and 9 August, two strong CCKWs are observed to propagate eastward across tropical Africa. The high-resolution TRMM 3B42 product shows that the higher-amplitude rain-rate anomalies that occur within the convective envelopes of both CCKWs are associated with westward-propagating convective disturbances. In contrast to the convectively active phase, the convectively suppressed phases of both CCKWs (dashed black contours) are associated with reduced rain-rate anomalies. Therefore, during the analysis period, a suppressed–enhanced–suppressed–enhanced–suppressed sequence of unfiltered anomalous rain rates is clearly visible within the westward-propagating MCSs over Africa. It is evident from Fig. 1 that rainfall patterns during this period over Africa were highly influenced by CCKW activity.

The anomalous rain-rate signature associated with the MCS linked to the genesis of the pre-Alberto AEW originates on 30 July over the Darfur Mountains ($\sim$25°E), consistent with the observations of Berry and Thorncroft (2005). The initiation of this MCS occurred roughly 15° of longitude to the east of the maximum Kelvin-filtered TRMM rain-rate anomaly. Past research has shown that the maximum low-level zonal wind convergence associated with CCKWs is located about 15° of longitude to the east of the center of the convective envelope (Takayabu and Murakami 1994; Straub and Kiladis 2003a,b). Therefore, this MCS developed in a region relative to the CCKW that was associated with increased low-level zonal wind convergence and vertical ascent (not shown). One day later (31 July), 700-hPa southerly winds associated with the pre-Alberto AEW circulation developed during the passage of the CCKW, indicating when the dynamical signature associated with the AEW had begun.

Between 30 and 31 July, the pre-Alberto AEW was still superimposed with the convective envelope of the first CCKW. During this time, the pre-Alberto AEW had an anomalous rain-rate signature greater than 40 mm day^{-1}. By 1 August, the pre-Alberto AEW was collocated with the convectively suppressed phase of the CCKW. During the superposition, the anomalous rain-rate signature associated with the pre-Alberto AEW weakened. Note that this convectively suppressed CCKW phase reduced rain-rate anomalies to zero for other preexisting westward-moving MCSs over Africa.

The superposition between the pre-Alberto AEW and the convectively active phase of the following CCKW occurred between 1 and 2 August around 10°W–0°.

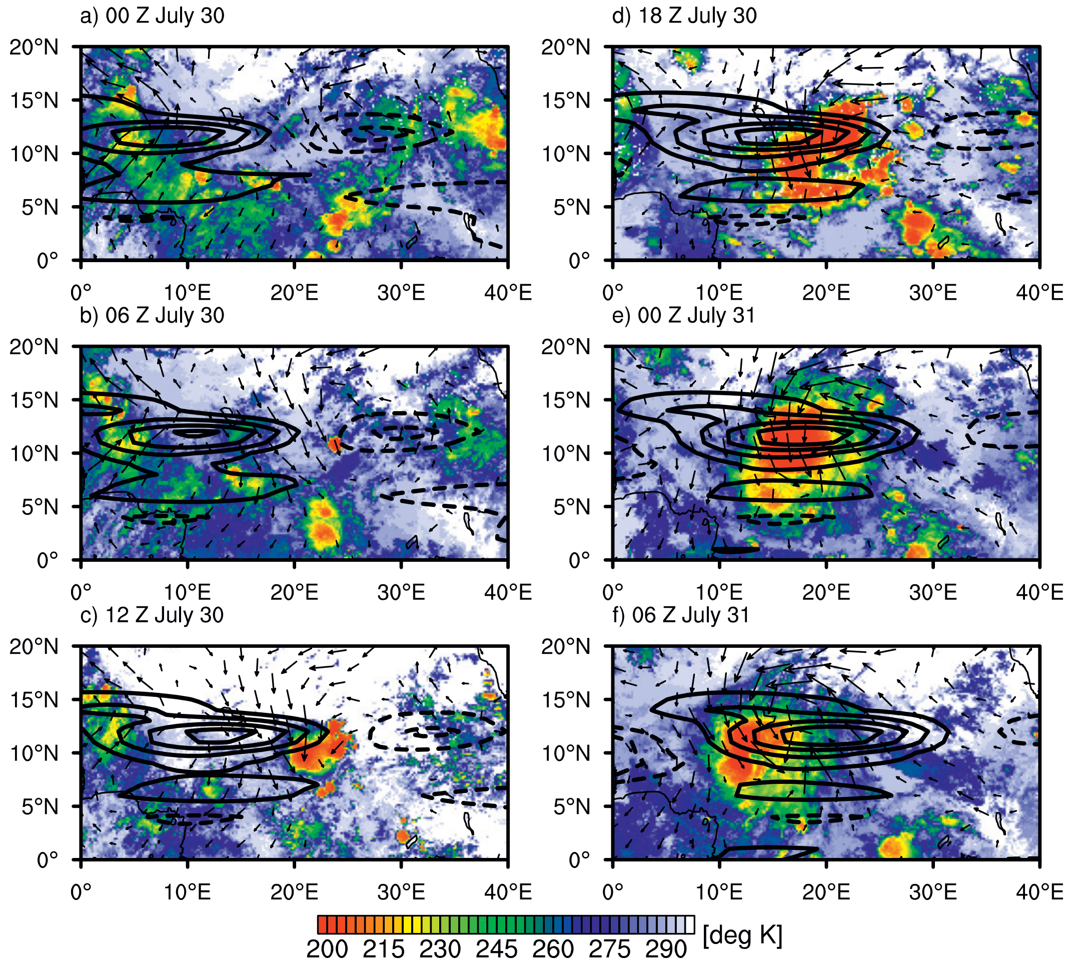

FIG. 2. Infrared radiation (shaded) overlaid with Kelvin-filtered rain-rate anomalies (black contours) and 850-hPa wind anomalies (vectors) for the period 1800 UTC 29 Jul–0600 UTC 31 Jul 2000. The shading interval is 2.5 K, the contour interval is 3 mm day^{-1}, and the reference vector is 10 m s^{-1}.

During this time, the anomalous rain-rate signature associated with the pre-Alberto AEW increased to values greater than 40 mm day^{-1} again. At this time, Berry and Thorncroft (2005) note the merging between low-level PV generated over the Guinea Highlands region (5°–13°N, 8°–15°W) with the pre-Alberto AEW. The low-level PV generated over the Guinea Highlands region was presumed to be generated with a coherent diurnal cycle there. Berry and Thorncroft (2005) deemed this as the final stage of an AEW life cycle and called it the ''west coast development'' stage. While AEWs may intensify over western tropical Africa from local processes, it is suggested that the intensification of the pre-Alberto AEW over western Africa was also in association with the superposition of the convectively active phase of an eastward-propagating CCKW.

To investigate the initiation of the pre-Alberto AEW in greater detail, maps of CPC-merged IR (shaded) overlaid with Kelvin-filtered TRMM anomalies (black contours) and ERA-interim 850-hPa wind anomalies (vectors) are constructed every 6 h for the period beginning at 0000 UTC 30 July and ending 0600 UTC 31 July (Fig. 2). The domain of Fig. 2 is focused over eastern Africa, where the northeastern extent of the Gulf of Guinea is located in the bottom-left corner. At 0000 UTC 30 July, the convectively active phase of the leading CCKW is located between 0° and 15°E, while its convectively suppressed phase is located between 25° and 30°E. Note that scattered MCSs were present across eastern Africa at this time, consistent with a time of day when convection is found most frequent there (Yang and Slingo 2001; Laing et al. 2008, 2011). By 0600 UTC 30 July, a small MCS developed over 11°N, 24°E, with a brightness temperature value that was less than 200 K, in between the convectively suppressed and active phases of the CCKW. Consistent with Fig. 1, this

MCS formed roughly 15° of longitude to the east of the maximum positive Kelvin-filtered TRMM rain-rate anomaly. The MCS formed during a time of day (0000–0600 UTC) when convection is on average suppressed, suggesting that forcing from the CCKW was able to overcome the forcing associated with the coherent diurnal cycle of convection. This MCS is found to be the leading convective disturbance associated with the pre-Alberto AEW (recall Fig. 1).

By 1200 UTC 30 July, the small MCS grew in horizontal extent and magnitude during the superposition with the eastwardmost edge of the convectively active phase of the CCKW (Fig. 2c). Note that the scattered preexisting MCSs over 30°–40°E weakened while superimposed with the convectively suppressed phase of the CCKW. These MCSs weakened during a time of day when convection is on average most frequent and remain in a suppressed state while superimposed with the convectively suppressed phase of the CCKW through 1800 UTC 30 July (Fig. 2d). By 1800 UTC 30 July, the pre-Alberto MCS is now centered about 20°E and is observed to further amplify and grow in horizontal extent while superimposed with the convectively active phase of the CCKW. At this time, easterly wind anomalies (over 5°–15°N, 25°–35°E) are observed to the east of the convectively active phase of the CCKW, whereas westerly wind anomalies (over 5°–10°N, 0°–5°E) are observed to its west. This low-level wind signature is consistent with the low-level wind structure of the CCKW over Africa (Mounier et al. 2007). However, northerly wind anomalies are also evident within the maximum positive Kelvin-filtered TRMM rain-rate anomaly. These northerly wind anomalies are attributed to the formation of the low-level wind signature of the pre-Alberto AEW, not the CCKW. Further at this time, the deepest convection is collocated with the northerly flow, consistent with the observed structure of an AEW over Africa (e.g., Carlson 1969a,b; Reed et al. 1977; Duvel 1990; Diedhiou et al. 1999; Payne and McGarry 1977; Fink and Reiner 2003; Kiladis et al. 2006). By 0000 UTC 31 July, the pre-Alberto AEW has shifted slightly westward while still superimposed with the western half of the convectively active phase of the CCKW (Fig. 2e). By 0600 UTC 31 July, deep convection associated with the AEW remained prominent while superimposed with the convectively active phase of the CCKW (Fig. 2f). This deep convection remained active during a time of day when convection is on average suppressed, suggesting that the combined forcing from the CCKW and the newly spawned AEW is greater than that of the forcing from the coherent diurnal cycle of convection over Africa.

Depending on the phase of the CCKW, rainfall is either increased or reduced over tropical Africa (e.g., Mounier et al. 2007; Mekonnen et al. 2008; Laing et al. 2011). The convectively active phase of the CCKW increases the amplitude and frequency of westward-moving MCSs, whereas the suppressed phase reduces both. In the pre-Alberto AEW case, the convectively suppressed phase of the leading CCKW may have contributed to the decay of the MCS on 29 July that Hill and Lin (2003) argue was important for the pre-Alberto AEW genesis over the Ethiopia Highlands (recall Fig. 1). The initiation of the MCS that Berry and Thorncroft (2005) argue later developed into the pre-Alberto AEW has been shown to occur during the passage of the convectively active phase of an eastward-propagating CCKW. This MCS amplified within the convectively active phase of the CCKW during a time of day when convection is expected to be active. However, this MCS also remained prominent while superimposed with the convectively active phase of the CCKW through 0600 UTC, a time of day where convection is on average suppressed over Darfur. A study comparing CCKWs and the diurnal cycle of convection within the tropics is needed to fully understand the role of the CCKW and diurnally varying convection but is beyond the scope of this study. Motivated by the results above, we now explore the climatological influence of CCKWs over tropical Africa in order to assess the extent to which AEWs are triggered generally and to better understand the physical reasons of why the pre-Alberto AEW initiated during the passage of the CCKW.

4. The climatological role of the convectively coupled Kelvin waves on the synoptic environment over Africa

The zonal wind anomaly structure of a composite CCKW has strong westward tilts in the lower troposphere, with upper-tropospheric winds generally opposite to those in the lower troposphere (e.g., Straub and Kiladis 2002; Kiladis et al. 2009; Ventrice et al. 2012b). Because of this vertical wind structure, CCKWs must influence the background low-level easterly vertical wind shear over tropical Africa during boreal summer. For example, the amplification of low-level easterly vertical wind shear over Africa could provide a favorable environment for the development of organized convection (e.g., Rotunno et al. 1988; Lafore and Moncrieff 1989). Further, since CCKWs strongly impact the zonal wind in the lower troposphere, we expect CCKWs to alter the nature of the midlevel AEJ. These parameters are now explored in turn to investigate the role of CCKWs on the synoptic environment important for convection and AEW growth over Africa.

a. 925–700-hPa vertical wind shear

The organization of ordinary convection into propagating MCSs is favored under moderate vertical wind shear of the horizontal wind (e.g., Rotunno et al. 1988; Lafore and Moncrieff 1989). Over Africa, Laing et al. (2008, 2011) found that frequent deep convection is associated with maxima in the 925–600-hPa easterly shear over northern tropical Africa during May–August. This low-level vertical wind shear varies day to day and comprises the low-level monsoon westerlies and the midlevel AEJ. Since CCKWs are characterized by strong westward vertical tilts with height of the zonal wind, both the 925- and 700-hPa zonal wind fields are strongly influenced by CCKW passages. Therefore, these waves must affect the low-level vertical wind shear over Africa.

Anomalies of 925–700-hPa vertical wind shear magnitude (shaded) and direction (vectors) are averaged over each lag of the CCKW index to investigate the influence of the CCKW on low-level shear over Africa (Fig. 3). The direction of shear represents the vector difference between 925 and 700 hPa. On day -1, the convectively suppressed phase of the CCKW is located over western tropical Africa, while its convectively active phase is located over the eastern tropical Atlantic (Fig. 3a). Anomalous easterly shear extends from the western half of the convectively suppressed phase of the CCKW through the convectively active phase, covering over 30° of longitude. This anomalous easterly shear adds 0.5–1 m s^{-1} to the background easterly shear over Africa. Northeast of the convectively suppressed phase of the CCKW is a small area of anomalous westerly shear. The anomalous westerly shear is created by anomalous low-level (850 hPa and below) easterly flow associated with the convectively suppressed phase of the CCKW, where easterly anomalies weaken above 850 hPa. This anomalous westerly shear is collocated with the convectively suppressed phase of the CCKW and reduces the background low-level easterly vertical wind shear over Africa during the next two days (Figs. 3b,c).

By day 0, the convectively active phase of the CCKW is located over the coast of West Africa (Fig. 3b). Anomalous easterly vertical wind shear is collocated with the convectively active phase of the CCKW, which increases the background easterly vertical wind shear there. In addition to occurring within the convectively active phase of the CCKW, significant anomalous easterly shear extends eastward to the maximum positive Kelvin-filtered OLR anomaly. Note that in addition to the convectively active phase of the CCKW, the area in between the leading suppressed phase and the

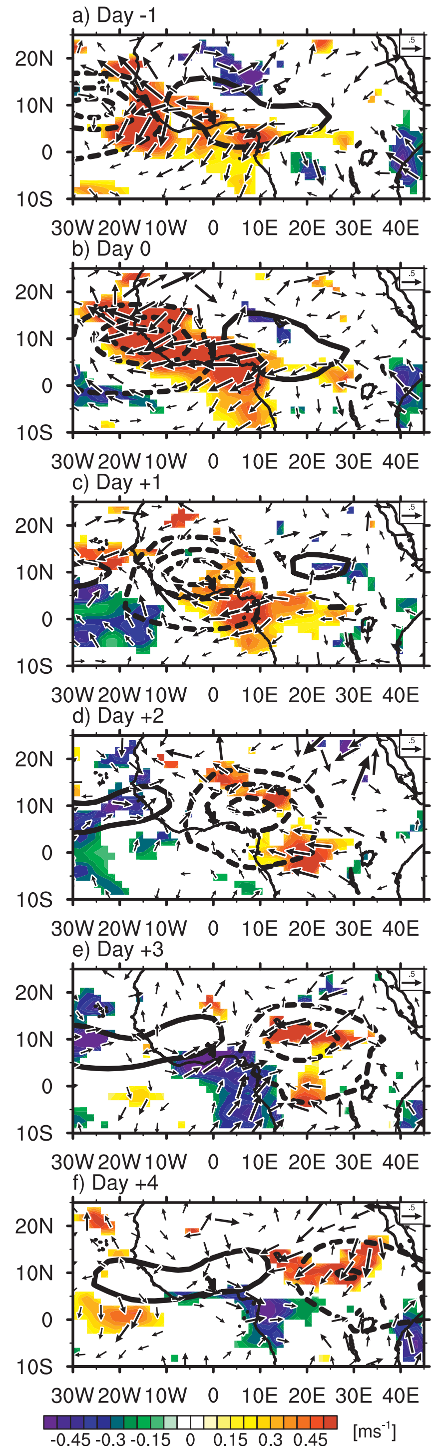

FIG. 3. The 925–700-hPa vertical wind shear vector and magnitude (shaded) anomaly composite averaged over each CCKW lag. Wind shear magnitude anomalies statistically different than zero at the 90% level are shaded. Vectors represent the vector difference between 925 and 700 hPa. Kelvin-filtered OLR anomalies are contoured if statistically different than zero at the 95% level. Negative Kelvin-filtered OLR anomalies are dashed. The shading interval is 0.1 m s^{-1}, the contour interval is 3 W m^{-2}, and the reference shear vector is 0.5 m s^{-1}.

convectively active phase of the CCKW is also an environment that favors the development of organized convection because of the enhancement of background low-level easterly shear there (e.g., Laing et al. 2008, 2011). A vertical cross section of anomalous zonal wind on day 0 over the longitude at 8.5°N shows that the increased easterly vertical wind shear in between the leading convectively suppressed phase and the active phase of the CCKW (0°–10°W) is primarily driven by anomalous easterly winds extending back toward the west with height (Fig. 4). The anomalous easterly shear within the convectively active phase of the CCKW (0°–25°W) is from the combination of midtropospheric easterly flow undercut by anomalous westerly flow.

Between days +1 and +4, anomalous easterly vertical wind shear progresses eastward with the convectively active phase of the CCKW (Figs. 3c–f). Following this convectively active phase of the CCKW is its suppressed phase, which is associated with anomalous westerly vertical wind shear. Between days +1 and +4, this anomalous westerly vertical wind shear reduces the background easterly vertical wind shear over the equatorial Atlantic and Africa by roughly 0.5 m s^{-1} (Figs. 3c–f).

By increasing the background low-level easterly vertical wind shear over Africa, the CCKW provides an environment known to be favorable for the organization of ordinary convection into propagating MCSs. This increased vertical wind occurs within the convectively active phase of the CCKW, but increased vertical wind shear also occurs just ahead of it. The more frequent, stronger MCS activity within the easterly low-level vertical wind sheared phase of the CCKW also increases the likelihood of initiating AEWs or intensifying preexisting AEWs (e.g., Thorncroft et al. 2008). Recall that the MCS that later developed into the pre-Alberto AEW formed in between the leading convectively suppressed phase and convectively active phase of a CCKW, indicative that it formed in a region relative to the CCKW where low-level vertical wind shear was enhanced (Fig. 2c). This MCS grew during the passage of the convectively active phase of the CCKW, consistent with the region relative to CCKW where increased low-level easterly vertical low-level wind shear is present.

b. *The impact of convectively coupled Kelvin waves on the horizontal structure of the African easterly jet*

Fields of total 700-hPa easterly winds (dashed contours), anomalies of 700-hPa zonal wind (shaded), and Kelvin-filtered OLR anomalies (bold contours) are averaged over each lag of the CCKW index to investigate the impact of the CCKW passage on the horizontal structure of the AEJ (Fig. 5). Easterly 700-hPa wind anomalies generally occur within the convectively suppressed phase of the CCKW (see Fig. 4). These easterly anomalies also extend westward through the eastwardmost edge of the convectively active phase, consistent with the westward vertical tilted structure of the CCKW. Anomalous westerly winds follow the minimum negative Kelvin-filtered OLR anomaly (Figs. 5d–l). These anomalous westerly winds extend westward through the following convectively suppressed phase of the CCKW (Figs. 5h,i), again consistent with the westerly tilt of the winds. It is important to comment on the anomalous easterly wind signature over the Atlantic between days −4 and −2 (Figs. 5c–e). During this time, there are easterly anomalies collocated within the convectively active phase of the CCKW. This signature is not representative of the expected structure of the CCKW and is associated with an interference pattern caused by a westward moving signature that has been attributed to a Saharan air layer (SAL) outbreak across the tropical Atlantic between days −6 and 0 (Ventrice et al. 2012b).

The AEJ can be modulated by the CCKW in two main ways. The first is associated with the equatorial wind structure of the CCKW, which can modulate the horizontal shear of the AEJ on the equatorward side (e.g., Matthews 2004). The second process is associated with convection generated by the CCKW over Africa. Following the argument of Thorncroft and Blackburn (1999), increased convection on the equatorward side of the jet generates PV near the level of the jet, acting to strengthen the jet. On day −6, the highest-amplitude easterly winds associated with the AEJ are located over West Africa and centered over the coast of West Africa, indicated by the −9 m s^{-1} isotach (Fig. 6a). Between days −5 and −2, the −9 m s^{-1} isotach extends westward

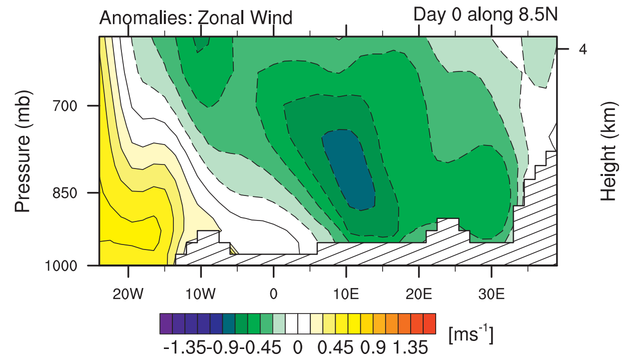

FIG. 4. A height–longitude composite of zonal wind anomalies along 8°N on day 0 of the CCKW index. The slanted black lines on white fill represents the topography of West Africa.

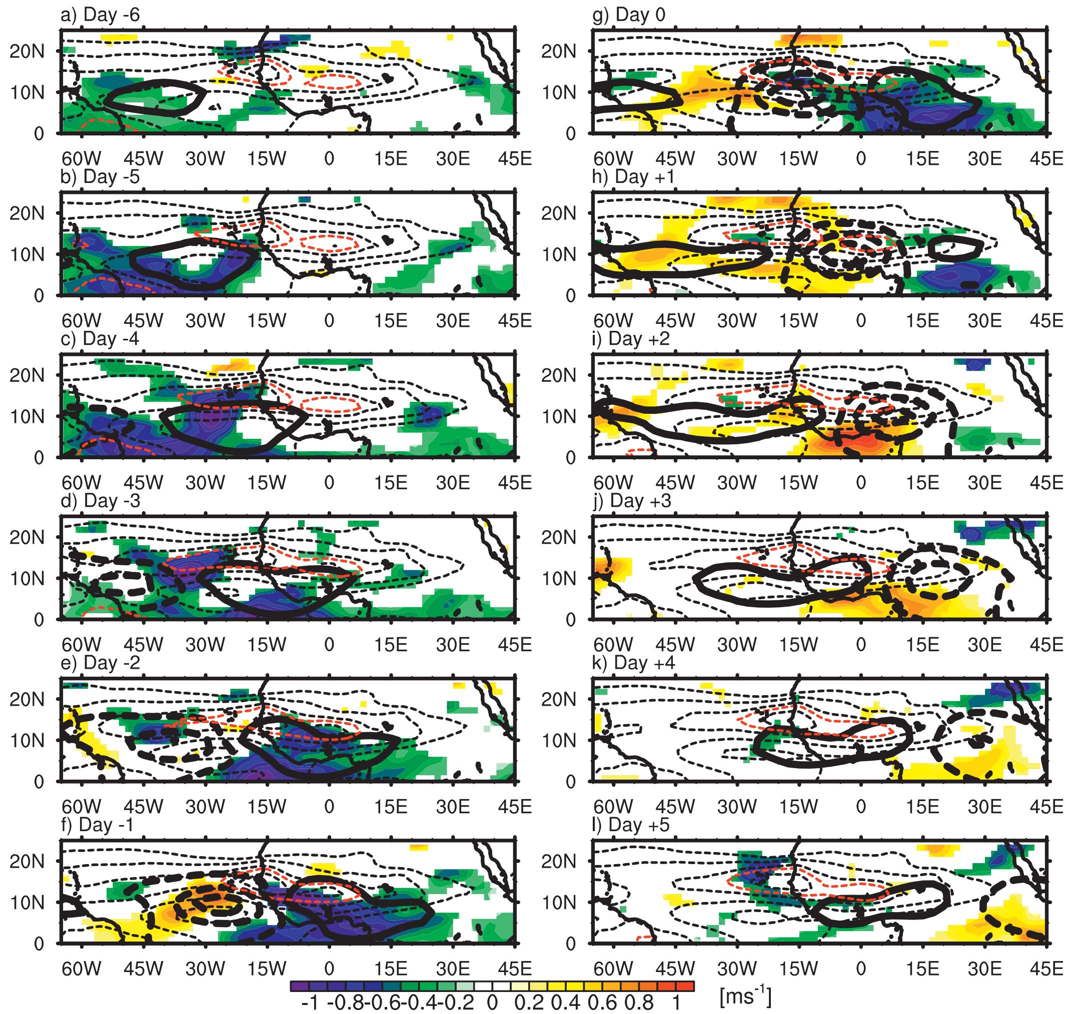

FIG. 5. 700-hPa zonal wind anomalies averaged over each CCKW lag. Anomalies statistically different than zero at the 95% level are shaded. Total raw easterly zonal wind is composited for each CCKW lag and contoured. Kelvin-filtered OLR anomalies are contoured (bold). The shading interval is 0.2 m s^{-1}, the Kelvin-filtered OLR contour interval is 3 W m^{-2}, the easterly 700-hPa winds contour range from -10 to -4 m s^{-1}, and the wind contour interval is 2 m s^{-1}. The red dashed contour highlights the -9 m s^{-1} contour.

over the central tropical Atlantic (to ~40°W), highlighting a westward extension of the AEJ (Figs. 6b–e). This westward extension of the jet over the tropical Atlantic separates moist monsoonal air equatorward of the jet, and a dry SAL poleward of it. Consistent with these observations, Ventrice et al. (2012b) found that an area of anomalously dry air progressed westward across the northern tropical Atlantic during the passage of the convectively active phase of a CCKW.

Over Africa, the 700-hPa easterly wind anomalies associated with the convectively suppressed phase of the CCKW increase the total magnitude of the AEJ between days -4 and $+1$ (Figs. 5c–h). Between days -1 and $+1$, Kelvin wave–induced easterly anomalies accelerate the upstream half of the AEJ, extending the jet entrance region eastward over the Darfur Mountains. Previous literature that has focused on the intraseasonal variability of AEW activity (e.g., Leroux et al. 2010; Ventrice et al. 2011; Alaka and Maloney 2012) have shown that an eastward extension of the AEJ entrance region over the Darfur Mountains precedes a period of increased AEW activity. We hypothesize that the eastward extension of the AEJ entrance region will increase barotropic and baroclinic energy conversions for AEW growth over the Darfur Mountains and Ethiopian Highlands. Therefore, the convectively suppressed phase of the CCKW may reinforce the upstream half of the AEJ to precondition, or "load" the jet for a future period of increased AEW activity. These easterly wind anomalies are present for about four days and so whether these exist

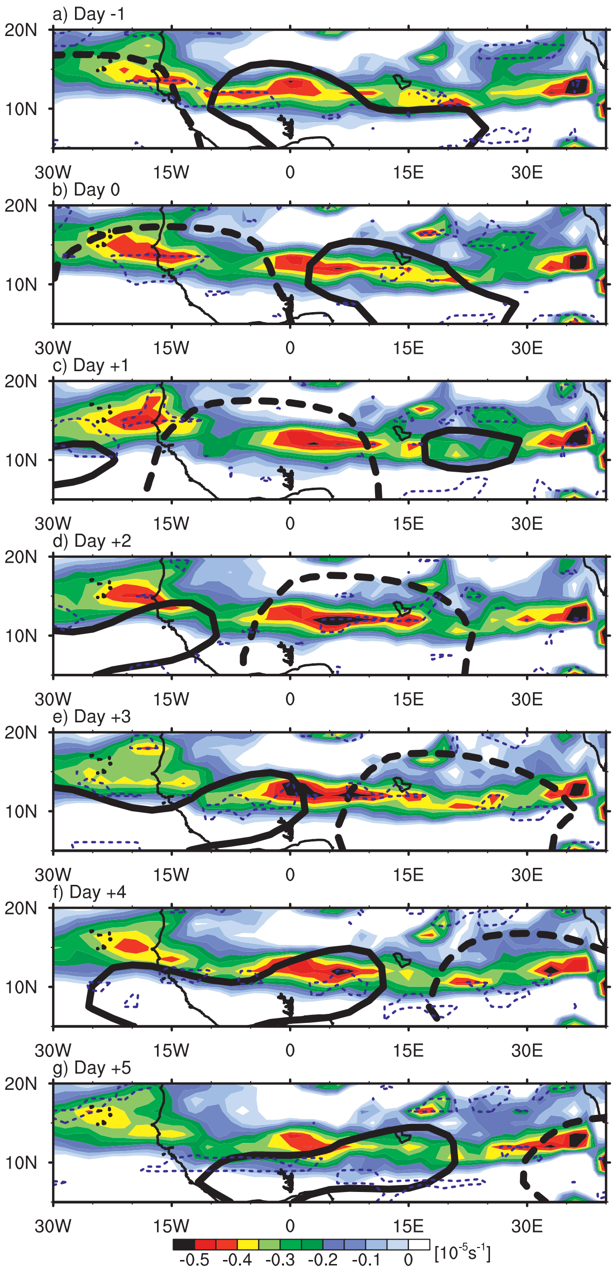

FIG. 6. The negative meridional gradient of 700-hPa absolute vorticity (shaded) averaged over each CCKW lag. Negative anomalies of the meridional negative gradient of absolute vorticity that are statistically different than zero at the 95% level are represented by the blue dashed contours. Kelvin-filtered OLR anomalies are contoured black (dashed if negative). The shading interval is 0.05 10^{-5} s^{-1} and the ± 3 W m^{-2} Kelvin-filtered OLR anomalies are only drawn.

long enough to influence the subsequent AEW activity is an open question that should be investigated in future work.

For all days in Fig. 5, the maximum zonal wind anomaly is generally peaked equatorward of the AEJ. This signature suggests that the CCKW is affecting the horizontal shear across the AEJ, which modifies the vorticity sign reversal in the jet core. A tighter horizontal gradient of easterly zonal wind is indicative of a more unstable AEJ, and vice versa. To verify that the CCKW's impact on the horizontal shear of the AEJ is significant enough to affect the meridional gradient of vorticity over Africa, Fig. 6 shows the negative gradient of 700-hPa absolute vorticity (hereafter NGAV; shaded) averaged over each CCKW lag between days −1 and +5. Areas where the NGAV is anomalously more negative, such that it is statistically different than zero at the 95% level, are represented by the blue dashed contour. To clarify, the collocation of significant NGAV anomalies and the raw NGAV strip can be interpreted as the AEJ becoming significantly more unstable. On day −1, the AEJ is more unstable over western tropical Africa between 20°W–0° during the passage of the convectively active phase of the CCKW (consistent with anomalous westerlies on the equatorward side of the AEJ), and over eastern Africa between 16°–22°E during the passage of the its suppressed phase (consistent with an eastward extension of the AEJ there as seen in Fig. 5f). Over western Africa, the AEJ is anomalously unstable through day +2, or two days after the passage of the convectively active phase of the CCKW (Figs. 6b–d).

By day +2, the AEJ is more unstable over central tropical Africa (5°–18°E) during the passage of the convectively active phase of the CCKW. The AEJ over central Africa remains anomalously unstable up to two days after the passage of the convectively active phase of the CCKW (until day +4; Figs. 6d–f). Between days +3 and +5, significant NGAV anomalies are collocated with the raw NGAV strip over eastern tropical Africa (20°–30°E) during, and just after, the passage of the convectively active phase of the CCKW. This result suggests that the AEJ is more unstable over the "trigger region" during this time (Figs. 6e–g).

The combined effect of enhanced convection and anomalous 700-hPa westerly winds associated with the convectively active phase of the CCKW increases the instability of the AEJ during and up to two days after its passage. While the AEJ becomes more unstable during the passage of the convectively active phase of the CCKW, moist convection triggered by the CCKW is assumed to play a prominent role with regards to modulating AEW activity over Africa.

c. 2–10-day filtered eddy kinetic energy

The convectively active phase of the CCKW is assumed to increase AEW activity by increasing the number of strong and long-lasting MCSs over Africa that can serve as convective triggers (e.g., Mounier et al. 2007; Nguyen and Duvel 2008; Laing et al. 2011). These MCSs thrive in an environment characterized by increased low-level easterly shear, which then propagate back toward the west within a more unstable AEJ.

A time–longitude composite of 2–10-day filtered daily averaged EKE anomalies composited over each lag of the CCKW index shows the relationship between CCKWs and AEW activity (Fig. 7). Recall that day 0 is when the minimum Kelvin-filtered OLR anomaly is located over the base point (10°N, 15°W). Between days −5 and +2, no significant positive EKE anomalies develop over the tropical Atlantic during the passage of the convectively active phase of the CCKW. Positive EKE anomalies first develop over West Africa (15°W–0°) after the passage of the convectively active phase of the CCKW over the coast of West Africa. This result suggests that the convectively active phase of the CCKW is insufficient alone to modulate easterly wave activity without the presence of the AEJ and African topography. Positive EKE anomalies are generated directly after the passage of the convectively active phase of the CCKW over western tropical Africa (between 20°W and 0°). Thereafter, this large area of positive EKE anomalies over West Africa progresses westward over the Atlantic with an average phase speed of 9.0 m s^{-1}, consistent with the phase speed of an AEW (e.g., Kiladis et al. 2006, and references therein). We hypothesize that this anomalous EKE signature comprises many instances where preexisting AEWs are becoming stronger after the passage of the convectively active phase of the CCKW, similar to the pre-Alberto case in 2000 and the pre-Debby AEW case in 2006 (Ventrice et al. 2012a).

Positive EKE anomalies also develop over the Darfur Mountains (25°E) and over and downstream of the Ethiopian Highlands (30°–35°E) during the passage of the easternmost edge of the convectively active phase of the CCKW between days +2 and +3. Recall that the wind signature associated with the pre-Alberto AEW formed within the convectively active phase of the CCKW over the Darfur Mountains (Fig. 1). The positive EKE anomalies generated over the Darfur Mountains amplify within the convectively active phase of the CCKW and progress westward on time scales consistent with AEWs directly after the passage. This area of positive EKE anomalies progresses westward across tropical Africa between days +6 and +10 and over the tropical Atlantic thereafter.

Interestingly on day −1, significant positive EKE anomalies are generated over 20°–30°E prior to and during the passage of the convectively suppressed phase

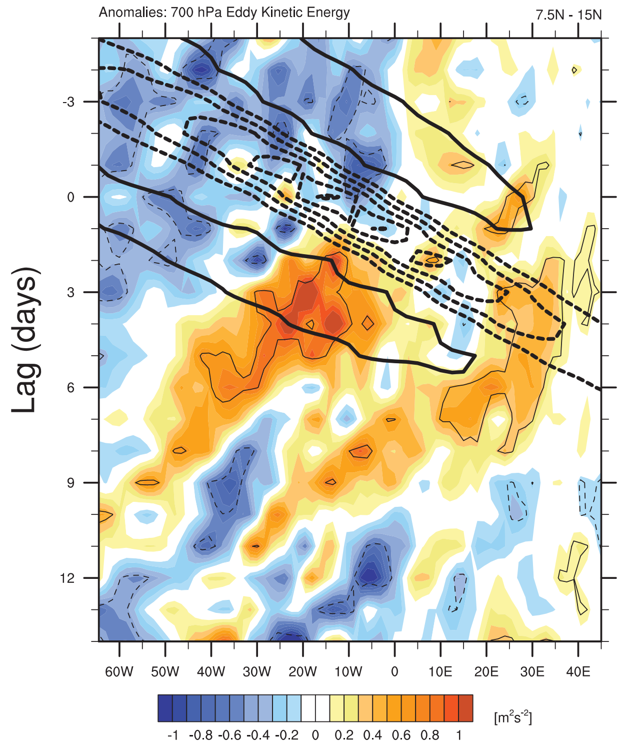

FIG. 7. A time–longitude composite of 2–10-day-filtered daily averaged 700-hPa eddy kinetic energy (shaded) averaged and over each lag of the CCKW index between the 7.5° and 15°N band. Positive (negative) eddy kinetic energy anomalies statistically different than zero at the 90% level are within the solid (dashed) contour. Kelvin-filtered OLR anomalies are averaged over the 5°–10°N latitude band and are contoured with bold lines. Negative Kelvin-filtered OLR anomalies are dashed. The shading interval is 0.1 $m^2 s^{-2}$ and the contour interval is 3 W m^{-2}.

of the CCKW. Recall that this is when the entrance region of the AEJ extends eastward over the eastern highlands of Africa (Fig. 5f). Therefore, any diurnally driven MCSs generated over the Darfur Mountains and Ethiopian Highlands prior to the passage of the convectively suppressed phase of the CCKW over might be sufficient enough to trigger an AEW due to the increased barotropic and baroclinic energy conversions associated with the eastward shifted jet. Further work is needed on the role of CCKWs and the eastward-shifted AEJ over the eastern African Highlands and their combined impact on AEW activity.

The enhancement of AEW activity during after the passage of the convectively active phase of the CCKW compares well to Fig. 14 in Mekonnen et al. (2008). In contrast to the suggestion of Mekonnen et al. (2008) that this was a rare event, the analysis presented here shows a coherent relationship between CCKWs and AEW activity.

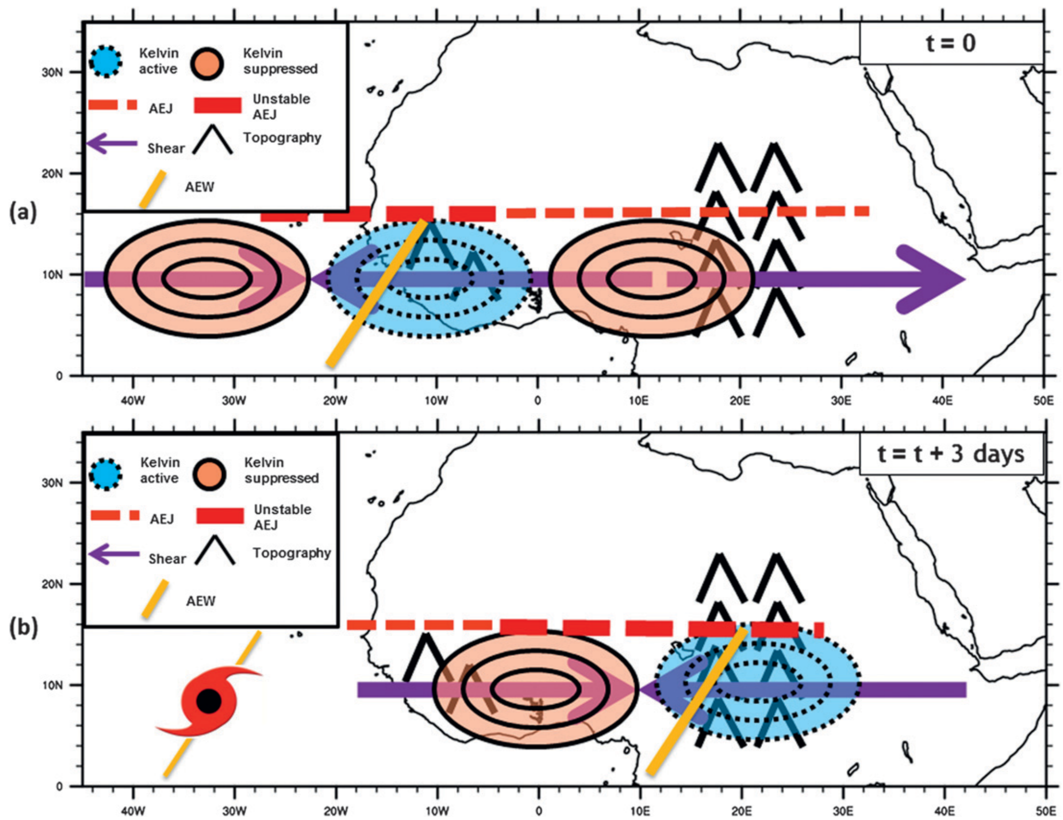

FIG. 8. A schematic diagram representing the modulation of the African environment and AEW activity by the passage of a CCKW when the convective envelope of the CCKW is over (a) the Guinea Highlands and (b) approximately three days later when it is over the eastern African Highlands.

5. Discussion and conclusions

This study shows evidence that CCKWs modulate AEW activity on synoptic time scales over West Africa during boreal summer. A TRMM 3B42 rain-rate anomaly time–longitude plot showed that the initiation of the pre-Alberto AEW (2000) occurred during the passage of a CCKW (Fig. 1). The convection attributed to the genesis of the pre-Alberto AEW described by Berry and Thorncroft (2005) was likely triggered by the passage of an eastward-propagating CCKW. It has been shown that a series of consecutive CCKWs strongly influenced the pre-Alberto AEW over Africa. We have also shown that the initiation and west coast developing stages (e.g., Berry and Thorncroft 2005) of the pre-Alberto AEW were times when it was superposed with the convectively active phases of subsequent CCKWs.

The convectively active phase of CCKWs modulates the synoptic environment over tropical Africa through convective and dynamical processes that provide a favorable environment for increasing AEW activity. Figure 8 shows two schematic diagrams characterizing the evolution of the environment over Africa during the passage of a CCKW over West Africa at arbitrary times $t = 0$ (when the active phase of the CCKW is over the Guinea Highlands) and $t = t + 3$ days (when the active phase of the CCKW is over the eastern African Highlands). Beginning with time $t = 0$ (cf. day 0 in the composite analysis), the convectively active phase of the CCKW is located over the Guinea Highlands region in West Africa (Fig. 8a). Enhanced low-level easterly shear (purple arrow) extends from the convective envelope of the CCKW eastward to the center of its convectively suppressed phase, with anomalous low-level westerly shear ahead of this convectively suppressed phase. Since the low-level shear is climatologically easterly over Africa and is attributed to the combination of the midlevel AEJ and low-level monsoon westerlies, the Kelvin-induced low-level westerly shear that occurs just east of the leading suppressed phase of the CCKW reduces the background low-level easterly vertical wind shear. In contrast, the Kelvin-induced low-level easterly shear, which occurs within and immediately to the east of the convectively active phase of the CCKW, increases the background low-level easterly shear over Africa. The increased anomalous easterly shear generated by the CCKW is a known condition that is beneficial for strong and long-lasting MCS development (e.g., Mounier et al. 2007; Nguyen and Duvel 2008; Laing et al. 2011). By increasing the frequency of strong, long-lasting MCSs, the CCKW increases the likelihood of convective triggers over Africa and thus increases the chances of AEW initiation over the eastern African Highlands (e.g., Thorncroft et al. 2008).

The AEJ (red dashed line) becomes more unstable (thick dark red dashed line) over western Africa during the passage of the convectively active phase of the CCKW. Enhanced vorticity gradients in the AEJ region arise in association with a diabatically generated PV strip consistent with Schubert et al. (1991), Hsieh and Cook (2005), and Schreck and Molinari (2011). The enhanced vorticity gradients are also consistent with increased cyclonic shear due to the presence of CCKW-associated westerlies on the equatorward flank of the AEJ (consistent with Matthews 2004). CCKW-induced anomalous westerly flow at the level of the AEJ increases horizontal shear on the equatorward side of the AEJ, indicative of a more unstable jet. The more unstable jet is consistent with the time when convection is enhanced over Africa by the CCKW. Since the CCKW provides an environment associated with a more unstable AEJ and intense moist convection, a westward-propagating AEW response (orange slanted line) develops just after the passage of the convectively active phase of the CCKW over the Guinea Highlands region.

Roughly three days later (cf. day +3 in the composite analysis), the convective envelope associated with the CCKW is located over the Darfur Mountains (Fig. 8b). Enhanced low-level easterly shear propagates eastward with the CCKW, now providing a favorable environment for organized convection over the eastern African Highlands. Westerly wind anomalies at the level of the AEJ extend westward from the convectively active phase of the CCKW, increasing the horizontal shear on the equatorward side of the AEJ over the Congo region. Consistent with an environment favorable for AEW initiation and growth, a new AEW response develops over the eastern African Highlands during the passage of the convectively active phase of the CCKW. The AEW response to the CCKW passage over the Guinea Highlands region at time $t = 0$ has propagated back toward the west over the tropical Atlantic and becomes important to consider for Atlantic tropical cyclogenesis (e.g., Ventrice et al. 2012a,b).

An issue that needs to be addressed in future work is whether the eastward extension of the AEJ over the eastern African Highlands could be sufficient enough for AEW genesis even though there is local suppression forced by the CCKW. Further, is the subweekly period that the AEJ becomes more unstable in association with the passage of the convectively active phase of the CCKW long enough to aid in an extended period of enhanced AEW activity? Or does the common phasing with a lower-frequency mode, such as the MJO become important to consider (e.g., Ventrice et al. 2012b)? Such questions should be further studied using observations and models to better understand the variability of AEWs and MCSs in support of operational forecasting at daily to intraseasonal time scales.

In addition to boreal spring (e.g., Nguyen and Duvel 2008), CCKWs impact African weather variability during boreal summer. African forecasters should be aware of CCKWs for the direct impact on rainfall, as well as the triggering of AEWs over the Darfur Mountains, the Ethiopian Highlands, and even possibly the Guinean Highlands where east Atlantic tropical cyclogenesis implications become important to consider.

Acknowledgments. The authors would like thank NOAA/CPC, NCEP, and the NASA TRMM program for providing the satellite data in the study. We extend our gratitude to NASA for Grants NNX09AD08G and NNX10AU44G, which supported this research. Interpolated OLR data were provided by the NOAA/OAR/ESRL PSD, Boulder, Colorado (from their website online at http://www.esrl.noaa.gov/psd/). We would also like to thank NCAR for their support with NCL, which was used to generate the figures used in this manuscript.

REFERENCES

Alaka, G. J., and E. D. Maloney, 2012: The influence of the MJO on upstream precursors to African easterly waves. *J. Climate,* **25,** 3219–3236.

Avila, L. A., and R. J. Pasch, 1992: Atlantic tropical systems of 1991. *Mon. Wea. Rev.,* **120,** 2688–2696.

Berry, G., and C. D. Thorncroft, 2005: Case study of an intense African easterly wave. *Mon. Wea. Rev.,* **133,** 752–766.

Brown, D., R. Brownrigg, M. Haley, and W. Huang, 2012: The NCAR Command Language (NCL) (version 6.0.0). UCAR/NCAR Computational and Information Systems Laboratory, Boulder, CO. [Available online at http://dx.doi.org/10.5065/D6WD3XH5.]

Carlson, T. N., 1969a: Synoptic histories of three African disturbances that developed into Atlantic hurricanes. *Mon. Wea. Rev.,* **97,** 256–276.

——, 1969b: Some remarks on African disturbances and their progress over the tropical Atlantic. *Mon. Wea. Rev.,* **97,** 716–726.

Dee, D. P., and Coauthors, 2011: The ERA-Interim reanalysis: Configuration and performance of the data assimilation system. *Quart. J. Roy. Meteor. Soc.,* **137,** 553–597, doi:10.1002/qj.828.

Diedhiou, A., S. Janicot, S. Viltard, and H. Laurent, 1999: Easterly wave regimes and associated convection over West Africa and the tropical Atlantic: Results from NCEP/NCAR and ECMWF reanalyses. *Climate Dyn.,* **15,** 795–822.

Duvel, J. P., 1990: Convection over tropical Africa and the Atlantic Ocean during northern summer. Part II: Modulation by easterly waves. *Mon. Wea. Rev.,* **118,** 1855–1868.

Fink, A. H., and A. Reiner, 2003: Spatiotemporal variability of the relation between African easterly waves and West African squall lines in 1998 and 1999. *J. Geophys. Res.,* **108,** 4332, doi:10.1029/2002JD002816.

Frank, N. L., 1970: Atlantic tropical systems of 1969. *Mon. Wea. Rev.,* **98,** 307–314.

Gruber, A., 1974: The wavenumber-frequency spectra of satellite-measured brightness in the tropics. *J. Atmos. Sci.,* **31,** 1675–1680.

Hall, N. M. J., G. N. Kiladis, and C. D. Thorncroft, 2006: Three dimensional structure of African easterly waves. Part II: Dynamical modes. *J. Atmos. Sci.,* **63,** 2231–2245.

Hill, C. M., and Y.-L. Lin, 2003: Initiation of a mesoscale convective complex over the Ethiopian highlands preceding the genesis of Hurricane Alberto (2000): A precursor to tropical cyclogenesis. *Geophys. Res. Lett.,* **30,** 1232, doi:10.1029/2002GL016655.

Hsieh, J.-H., and K. H. Cook, 2005: Generation of African easterly wave disturbances: Relationship to the African easterly jet. *Mon. Wea. Rev.,* **133,** 1311–1327.

——, and ——, 2008: On the instability of the African easterly jet and the generation of African waves: Reversals of the potential vorticity gradient. *J. Atmos. Sci.,* **65,** 2130–2151.

Huffman, G. J., and Coauthors, 2007: The TRMM Multisatellite Precipitation Analysis (TMPA): Quasi-global, multiyear, combined-sensor precipitation estimates at fine scales. *J. Hydrometeor.,* **8,** 38–55.

Janowiak, R., R. J. Joyce, and Y. Yarosh, 2001: A real-time global half-hourly pixel- resolution infrared dataset and its applications. *Bull. Amer. Meteor. Soc.,* **82,** 205–217.

Kiladis, G. N., C. D. Thorncroft, and N. M. J. Hall, 2006: Three dimensional structure and dynamics of African easterly waves. Part I: Observations. *J. Atmos. Sci.,* **63,** 2212–2230.

——, M. C. Wheeler, P. T. Haertel, K. H. Straub, and P. E. Roundy, 2009: Convectively coupled equatorial waves. *Rev. Geophys.,* **47,** RG2003, doi:10.1029/2008RG000266.

Lafore, J.-P., and M. W. Moncrieff, 1989: A numerical investigation of the organization and interactions of the convective and stratiform regions of tropical squall lines. *J. Atmos. Sci.,* **46,** 521–544.

Laing, A. G., R. E. Carbone, V. Levizzani, and J. D. Tuttle, 2008: The propagation and diurnal cycles of deep convection in northern tropical Africa. *Quart. J. Roy. Meteor. Soc.,* **134,** 93–109.

——, ——, and ——, 2011: Cycles and propagation of deep convection over equatorial Africa. *Mon. Wea. Rev.,* **139,** 2832–2853.

Leroux, S., N. M. Hall, and G. N. Kiladis, 2010: A climatological study of transient–mean–flow interactions over West Africa. *Quart. J. Roy. Meteor. Soc.,* **136,** 397–410.

Liebmann, B., and C. A. Smith, 1996: Description of a complete (interpolated) outgoing longwave radiation dataset. *Bull. Amer. Meteor. Soc.,* **77,** 1275–1277.

Matthews, A. J., 2004: Intraseasonal variability over tropical Africa during northern summer. *J. Climate,* **17,** 2427–2440.

Mekonnen, A., C. D. Thorncroft, and A. R. Aiyyer, 2006: Analysis of convection and its association with African easterly waves. *J. Climate,* **19,** 5405–5421.

——, ——, ——, and G. N. Kiladis, 2008: Convectively coupled Kelvin waves over tropical Africa during the boreal summer: Structure and variability. *J. Climate,* **21,** 6649–6667.

Mounier, F., G. N. Kiladis, and S. Janicot, 2007: Analysis of the dominant mode of convectively coupled Kelvin waves in the West African monsoon. *J. Climate,* **20,** 1487–1503.

Nguyen, H., and J. P. Duvel, 2008: Synoptic wave perturbations and convective systems over equatorial Africa. *J. Climate,* **21,** 6372–6388.

Payne, S. W., and M. M. McGarry, 1977: The relationship of satellite inferred convective activity to easterly waves over West Africa and the adjacent ocean during phase III of GATE. *Mon. Wea. Rev.,* **105,** 414–420.

Pires, P., J.-L. Redelsperger, and J.-P. Lafore, 1997: Equatorial atmospheric waves and their association to convection. *Mon. Wea. Rev.,* **125,** 1167–1184.

Reed, J. R., D. C. Norquist, and E. E. Recker, 1977: The structure and properties of African wave disturbances as observed during phase III of GATE. *Mon. Wea. Rev.,* **105,** 317–333.

Rennick, M. A., 1976: The generation of African waves. *J. Atmos. Sci.,* **33,** 1955–1969.

Rotunno, R., J. B. Klemp, and M. L. Weisman, 1988: A theory for strong, long-lived squall lines. *J. Atmos. Sci.,* **45,** 463–485.

Roundy, P. E., and W. M. Frank, 2004: A climatology of waves in the equatorial region. *J. Atmos. Sci.,* **61,** 2105–2132.

Schreck, C. J., III, and J. Molinari, 2011: Tropical cyclogenesis associated with Kelvin waves and the Madden–Julian oscillation. *Mon. Wea. Rev.,* **139,** 2723–2734.

——, ——, and K. I. Mohr, 2011: Attributing tropical cyclogenesis to equatorial waves in the western North Pacific. *J. Atmos. Sci.,* **68,** 195–209.

Schubert, W. H., P. E. Stevens, and H. C. Kuo, 1991: Potential vorticity modeling of the ITCZ and the Hadley circulation. *J. Atmos. Sci.,* **48,** 1493–1509.

Simmons, A. J., 1977: A note on the instability of the African easterly jet. *J. Atmos. Sci.,* **34,** 1670–1674.

Straub, K. H., and G. N. Kiladis, 2002: Observations of a convectively coupled Kelvin waves in the eastern Pacific ITCZ. *J. Atmos. Sci.,* **59,** 30–53.

——, and ——, 2003a: Extratropical forcing of convectively coupled Kelvin waves during austral winter. *J. Atmos. Sci.,* **60,** 526–543.

——, and ——, 2003b: The observed structure of convectively coupled Kelvin waves: Comparison with simple models of coupled wave instability. *J. Atmos. Sci.,* **60,** 1655–1668.

Takayabu, Y. N., 1991: The structure of super cloud clusters observed in 1–20 June 1986 and their relationship to easterly waves. *J. Meteor. Soc. Japan,* **69,** 105–125.

——, and M. Murakami, 1994: Large-scale cloud disturbances associated with equatorial waves. Part I: Spectral features of the cloud disturbances. *J. Meteor. Soc. Japan,* **72,** 433–448.

Thorncroft, C. D., and B. J. Hoskins, 1994a: An idealized study of African easterly waves. Part I: A linear view. *Quart. J. Roy. Meteor. Soc.,* **120,** 953–982.

——, and ——, 1994b: An idealized study of African easterly waves. Part II: A non linear view. *Quart. J. Roy. Meteor. Soc.,* **120,** 983–1015.

——, and M. Blackburn, 1999: Maintenance of the African easterly jet. *Quart. J. Roy. Meteor. Soc.,* **125,** 763–786.

——, N. M. Hall, and G. K. Kiladis, 2008: Three-dimensional structure and dynamics of African easterly waves. Part III: Genesis. *J. Atmos. Sci.,* **65,** 3596–3607.

Tulich, S. N., and G. N. Kiladis, 2012: Squall lines and convectively coupled gravity waves in the tropics: Why do most cloud systems propagate westward? *J. Atmos. Sci.,* **69,** 2995–3012.

Ventrice, M. J., C. D. Thorncroft, and P. E. Roundy, 2011: The Madden–Julian oscillation on African easterly waves and downstream tropical cyclogenesis. *Mon. Wea. Rev.,* **139,** 2704–2722.

——, ——, and M. A. Janiga, 2012a: Atlantic tropical cyclogenesis: A three-way interaction between an African easterly wave, diurnally varying convection, and a convectively coupled atmospheric Kelvin wave. *Mon. Wea. Rev.,* **140,** 1108–1124.

——, ——, and C. J. Schreck, 2012b: Impacts of convectively coupled Kelvin waves on environmental conditions associated with Atlantic tropical cyclogenesis. *Mon. Wea. Rev.,* **140,** 2198–2214.

Wheeler, M., and G. N. Kiladis, 1999: Convectively coupled equatorial waves: Analysis of clouds and temperature in the wavenumber–frequency domain. *J. Atmos. Sci.,* **56,** 374–399.

——, and H. H. Hendon, 2004: An all-season real-time multivariate MJO index: Development of an index for monitoring and prediction. *Mon. Wea. Rev.,* **132,** 1917–1932.

——, G. N. Kiladis, and P. J. Webster, 2000: Large-scale dynamical fields associated with convectively coupled equatorial waves. *J. Atmos. Sci.,* **57,** 613–640.

Yang, G., and J. Slingo, 2001: The diurnal cycle in the tropics. *Mon. Wea. Rev.,* **129,** 784–801.

Zangvil, A., 1975: Temporal and spatial behavior of large-scale disturbances in tropical cloudiness deduced from satellite brightness data. *Mon. Wea. Rev.,* **103,** 904–920.